

УДК 539.172.17

## NEUTRON DRIP LINE IN THE REGION OF O–Mg ISOTOPES

*Yu. S. Lutostansky*<sup>a</sup>, *S. M. Lukyanov*<sup>b</sup>, *Yu. E. Penionzhkevich*<sup>b</sup>, *M. V. Zverev*<sup>c</sup>

<sup>a</sup> Moscow Physical Engineering Institute, Moscow

<sup>b</sup> Joint Institute for Nuclear Research, Dubna

<sup>c</sup> Russian Research Centre «Kurchatov Institute», Moscow

The results of the last experiments (RIKEN, GANIL, Dubna) on the mapping of the neutron drip line in the oxygen–magnesium region are discussed. The analysis of stability and properties of the neutron drip-line isotopes from the O–Mg region are performed using self-consistent theory of finite Fermi systems (STFFS). Conclusion about the vanishing of  $N = 20$  and  $N = 28$  and appearance of the new nuclear magic numbers  $N = 16$  and  $N = 26$  is given.

Обсуждаются результаты последних экспериментов (RIKEN, GANIL, Дубна) по изучению нейтронно-избыточных ядер вблизи границ стабильности для изотопов кислорода, фтора, неона, натрия и магния. Анализ свойств этих ядер выполнен в рамках самосогласованной теории конечных ферми-систем (STFFS). Сделано заключение об исчезновении нейтронных оболочек  $N = 20$  и  $N = 28$  в этой области ядер и появлении новых  $N = 16$  и  $N = 26$ .

### INTRODUCTION

The study of properties of neutron-rich nuclei far from stability is one of the most interesting areas of modern research in nuclear physics. The progress in our knowledge of the properties of these nuclei has enormously broadened because of the new radioactive ion beam facilities and the development of very sophisticated fragment separator.

An interesting feature has been found in the light neutron-rich nuclei. Neutron-rich unstable nuclei with  $N \approx 20$  constitute a good example since establishment in 1975 [1]. The nuclei in this region are spectacular examples of shape coexistence between spherical and deformed configurations. For example,  $^{31}\text{Na}$  and  $^{32}\text{Mg}$  with  $N = 20$  were found to be deformed. This new region of deformation for  $N = 20$ – $28$  neutron-rich nuclei was discussed in 1987 [2], while analyzing the sodium isotopes properties. It was shown that deformation mixed single-particle neutron levels, destroyed standard shell structure and changed strongly neutron separation and binding energy of nuclei. As a result, the drip line in the region  $N = 20$ – $28$  is shifted by several mass units compared to expected spherical case.

Recent experiments at GANIL, MSU and RIKEN have been devoted to studying the stability of the neutron-rich nuclei with  $Z > 7$  and around  $N = 20$ . The variation of the shell gap and deformation as a function of  $N$  and  $Z$  could be a major challenger.

Among recent results of the neutron drip-line study in the region of elements from O to Mg, one can mention the experiments on the particle instability of neutron-rich oxygen isotopes  $^{26,27,28}\text{O}$  [3–6] and the discovery of particle stability of  $^{31}\text{Ne}$  [7] and  $^{31}\text{F}$  [8].

The appearance of the so-called «island of inversion» with respect to the particle stability of isotopes has been claimed through various theoretical predictions. In neutron-rich sodium isotopes this inversion was predicted and analyzed in [2]. A particular feature of nuclei in this region is the progressive development of the static deformation in spite of the expected effect of spherical stability due to the magic neutron number  $N = 20$  [11, 12]. However, the situation with  $N = 20$  drip-line nuclei is not so clear because there may be other physical reasons for destroying the magic besides the deformation.

A more clear picture is in  $N > 20$  area. It was argued that the deformation might lead to enhanced binding energies in some of yet undiscovered neutron-rich nuclei. The particle stability of  $^{31}\text{F}$  gives a strong evidence of the onset of the deformation in this region. One may expect that the drip line for the fluorine–magnesium elements could move far beyond the presently known boundaries. Therefore, there is a great interest in studying of nuclei in the region of neutron closure  $N = 28$ . Experimentally, the properties of  $^{44}\text{S}$  had been studied [13] and it was concluded there that the ground state of  $^{44}\text{S}$  is deformed. This result suggests a significant breaking of the  $N = 28$  closure for nuclei near  $^{44}\text{S}$ .

In this article we analyze also the nuclei near the neutron drip line in theoretical approach and compare our previous calculations [16] proposed in spherical self-consistent basis with analogous calculations made including deformation effects.

## 1. EXPERIMENTAL MAPPING OF THE NEUTRON DRIP LINE

New attempts to determine the neutron drip line for the F–Ne–Mg isotopes in the region of the neutron numbers  $N = 20–28$  were presented recently in the framework of RIKEN–Dubna and GANIL–Dubna collaborations [14, 15] using the fragment spectrometers: LISE 2000 at GANIL (France) and RIPS at RIKEN (Japan).

In particular, experiments were devoted to the direct observation of the  $^{31}\text{F}$ ,  $^{34}\text{Ne}$ ,  $^{37}\text{Na}$  and  $^{40}\text{Mg}$  nuclei among the products of a primary beam fragmentation. In both experiments the neutron-rich nuclei were searched for among the fragmentation products of  $^{48}\text{Ca}$  beams on tantalum targets. This neutron-rich beam and target were chosen to optimize the production rate of the drip-line nuclei. The world records of mean beam intensity of the  $^{48}\text{Ca}$  beam at values above 150 pnA were reached at these experiments.

The reaction fragments were collected and analyzed by the fragment spectrometers operated in an achromatic mode and at the maximum values of momentum acceptance (5 %) and maximum solid angles. To reduce the overall counting rate due to light isotopes, a wedge was placed at the momentum dispersive focal plane.

The standard identification method of the fragments via time of flight (ToF), energy loss ( $dE$ ) and total kinetic energy (TKE) was used. A multiwire proportional detector was placed in the dispersive plane spectrometer. This detector allowed one to measure the magnetic rigidity of each fragment via its position in the focal plane, improving the mass-to-charge resolution ( $A/Q$ ).

The results of these experiments are shown in Fig. 1. Isotopes  $^{34}\text{Ne}$  and  $^{37}\text{Na}$  were unambiguously identified by measuring the magnetic rigidity, time of flight, energy loss and total kinetic energy. So, both experiments [14, 15] give the very clear evidence for the particle stability of  $^{34}\text{Ne}$ ,  $^{37}\text{Na}$ .

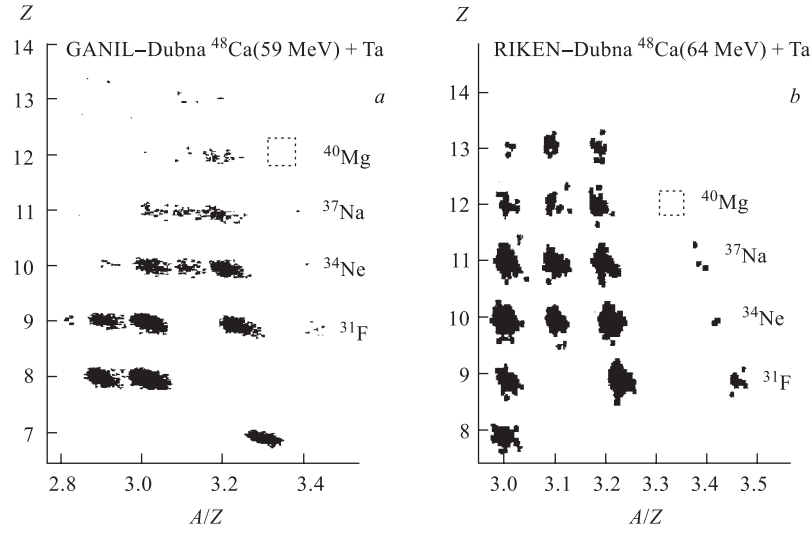


Fig. 1. Two-dimensional  $A/Z$  versus  $Z$  plot, which was obtained in the reaction of the  $^{48}\text{Ca}$  beam: a) at GANIL using the LISE-2000 spectrometer; b) at RIKEN using the RIPS spectrometer. Isotopes  $^{34}\text{Ne}$  and  $^{37}\text{Na}$  were unambiguously identified by measuring the magnetic rigidity, time of flight, energy loss and total kinetic energy. So, both experiments [14, 15] give the very clear evidences of the particle stability of  $^{34}\text{Ne}$ ,  $^{37}\text{Na}$

It was also found that particle instability of  $^{33}\text{Ne}$ ,  $^{36}\text{Na}$  and  $^{39}\text{Mg}$  was verified by the low background level.

The most interesting nuclide in this region is  $^{40}\text{Mg}$ , which is probably not bound, since no counts have been observed. The upper limit for the production cross-section of  $^{40}\text{Mg}$  to be less than 0.01 pb.

## 2. THEORETICAL APPROACH

From the theoretical point of view, the description of the light nuclei in the  $sd$ - $pf$  shells is still a problem. Various theoretical calculations (viz. finite-range liquid drop (FRLD) model [16], two versions of the shell model (SM) [17, 18], relativistic mean field theory [19], Hartree-Fock (HF) model [20] and relativistic Hartree + Bogoliubov (HF+B) description [21]) exist and predict the position of the neutron drip line in this region. For instance, the FRLD model gives a very strong binding energy for  $^{40}\text{Mg}$ . In the framework of this model, one- and two-neutron separation energies are even above 3.4 MeV. One may notice that the FRLD model gives correct predictions for stability of  $^{31}\text{Ne}$  and  $^{31}\text{F}$ , implying nuclear deformation effects for both the macroscopic and microscopic parts. According to the shell model predictions [17], the last bound isotopes are  $^{24}\text{O}$ ,  $^{27}\text{F}$ ,  $^{34}\text{Ne}$ ,  $^{37}\text{Na}$ , and  $^{38}\text{Mg}$ . However, slight changes of the drip line cannot be excluded since  $^{37}\text{Na}$  was predicted to be bound only by 250 keV, while  $^{31}\text{F}$  and  $^{40}\text{Mg}$  are unbound by 145, 470 and 550 keV, respectively. According to another shell model calculation [18],  $^{26}\text{O}$ ,  $^{34}\text{Ne}$  and  $^{40}\text{Mg}$  are the last stable isotopes against two-neutron emission, as indicated by their maximal binding

**Energies of separation of one ( $S_n$ ) and two ( $S_{2n}$ ) neutrons for nuclei near the neutron-stability boundary calculated in STFFS spherical basis**

$Z$	Nucleus	$N$	$S_n$ , MeV	$S_{2n}$ , MeV	Nucleus	$N$	$S_n$ , MeV ( $S_{2n} < 0$ )
8	$^{24}\text{O}$	16	3.59	5.85	$^{26}\text{O}$	18	0.69
9	$^{29}\text{F}$	20	1.64	0.90	$^{31}\text{F}$	22	< 0
10	$^{32}\text{Ne}$	22	1.65	0.33	$^{34}\text{Ne}$	24	0.16
11	$^{37}\text{Na}$	26	0.99	0.07	$^{39}\text{Na}$	28	< 0
12	$^{42}\text{Mg}$	30	1.13	0.38	$^{44}\text{Mg}$	32	0.91

energy. Both SM and HF calculations for even-mass O, Ne and Mg indicate a disappearance of shell magic numbers, and suggest an onset of the deformation and shape coexistence in this region.

We calculated properties of neutron drip-line isotopes from O–Mg region using self-consistent theory of finite Fermi systems (STFFS), specified by the quasiparticle Lagrangian which is a functional of four normal and one anomalous densities [22–25]. This Lagrangian is constructed in such a way that energy- and velocity-dependent two- and three-particle effective forces are taken into account in effective-range approximation. We use the approximation of volume pairing since all the characteristics under study, including the neutron-separation energy, are determined mainly by the gap operator  $\Delta$  diagonal elements which are weakly sensitive to the type of pairing [23, 24].

The results of STFFS calculations in spherical basis are shown in the table, which presents neutron separation energies  $S_n$  and  $S_{2n}$  calculated for extremely heavy stable isotopes that are  $N$ -even and the one-neutron-separation energies  $S_n$  found for the next  $N$ -even isotope. We can see that for even–even nuclei the position of the boundary in the considered region is determined by two-neutron instability. And as was predicted in [22] for  $^{26}\text{O}$ , a quasistationary state in  $^{24}\text{O} + 2n$  system may exist as  $^{26}\text{O}^*$  with the width  $\Gamma \sim 10^{-3}$  MeV. Analogously, for other extra drip-line nuclei of  $A$  (even–even) type,  $A^* = A + 2n$  quasistationary systems may exist, for example,  $^{36}\text{Ne}^*$  and  $^{40}\text{Mg}^*$ . The lifetime of such systems  $\tau \geq 10^{-18}$  s is much more than inner nuclear time  $\tau_{\text{nucl}} \sim 10^{-22}$  s and neutron pair should be emitting in a weakly bound di-neutron state.

From the table we can see that the results only for  $^{24}\text{O}$  and  $^{37}\text{Na}$  isotopes correspond to the experimental data. That is because of the fact that  $^{24}\text{O}$  isotope is spherical one and for  $^{37}\text{Na}$  due to the deformation effects the neutron drip-line number until  $\beta_2 < 0.4$  is  $N = 26$ , which corresponds particularly to the spherical basis calculations (see Fig. 3 and following discussion).

Deformation in STFFS may be taken into account as in [25] for axial type deformation for heavy and middle-mass nuclei, and in general as in [26], using very complicated energy-density functional approach. Here we estimate the influence of the quadrupole deformation using the approximation firstly mentioned in [2] (the details of the developed method will be soon published). In this method we estimate corrections  $\delta S_{2n}$  and  $\delta S_n$  as a function of quadrupole deformation parameter  $\beta_{20} = \beta_2$ . At the first stage, we calculate energetic parameters, single-particle levels  $\varepsilon_\lambda$  and wave functions in STFFS. At the second stage,

we calculate the influence of deformation on energetic parameters increasing  $\beta_2$  value step by step using  $\Delta\beta_2$ . In this approach we must calculate the single-particle levels scheme

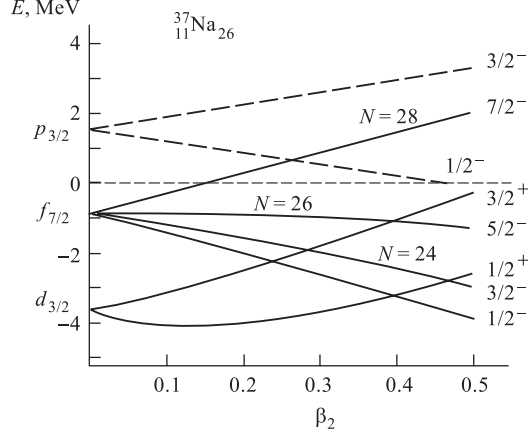


Fig. 2. Calculated single-particle levels scheme and wave functions, using an axially symmetric Saxon–Woods potential for different values of parameter  $\beta_2$  for  $^{37}\text{Na}$

using an axially symmetric Saxon–Woods potential for different values of parameter  $\beta_2$ . One of the results of such calculations of  $\varepsilon_\lambda = \varepsilon_\lambda(\beta_2)$  for  $^{37}\text{Na}$  presented in Fig.2 will be discussed later.

and wave functions, using an axially symmetric Saxon–Woods potential with the fixed parameter  $\beta_2 = \beta^i + \Delta\beta_2$ . Getting new wave functions and  $\varepsilon_\lambda$ , we may construct all necessary densities on axially symmetric basis. Solving STFFS equations with different values of parameter  $\beta_2$ , we find energetic parameters of nuclide and binding energy as functions of quadrupole deformation. Such calculations were performed earlier for sodium isotopes including  $^{35}\text{Na}$ , and the minimum of the binding energy, corresponding to the fixed  $\beta_2$  parameter, was found.

To analyze the role of deformation in our region of drip-line nuclei, we use here a simpler estimation. We calculate our nuclei in STFFS spherical basis as zero approximation and then we calculate their single-particle levels scheme and wave functions,

### 3. DISCUSSION

For the neutron-rich oxygen isotopes, deformation effects are negligible and we calculate them as spherical. Nevertheless, we analyzed deformation effects in  $Z = 8$  region. According to our estimations, when deformation is small ( $\beta_2 < 0.4$ ), good «magic» number for oxygen neutron-rich isotopes is  $N = 16$ . But in case of strong deformation with  $\beta_2 > 0.4$  the inverse level  $1/2^-$ , splitting down from  $f_{7/2}$  state, may form isomers with  $N = 18$ . So magic number  $N = 20$  is destroyed by the deformation. On the other hand, according to spherical STFFS calculations [22], strong pairing is developed in neutron system with  $N$  near 20 for very neutron-rich nuclei. This could be the main reason for destroying the magic  $N = 20$  in the considered region of nuclei.

Interesting picture can be seen for  $Z > 8$  drip-line nuclei. For fluorine and neon drip-line isotopes with deformation  $0.2 < \beta_2 < 0.4$ , the drip-line neutron number is  $N = 24$  corresponding to  $^{33}\text{F}$  and  $^{34}\text{Ne}$ . This means that an addition of only one  $Z$ -unit to  $Z = 8$  shifts the  $N$  drip line by eight neutrons, as illustrated on the map of nuclides in Fig.3. Comparing with the results of spherical calculations from the table, we can see in Fig.3 that due to deformation four neutrons are added to fluorine and two neutrons to neon drip-line isotopes. The question of  $^{36}\text{Ne}$  particle stability is still open in our approach because of uncertainties in the deformation and energetic parameters we use for  $\beta_2 > 0.4$ .

For the deformed sodium and magnesium, the neutron drip-line number is  $N = 26$ , which corresponds to  $^{37}\text{Na}$  and  $^{38}\text{Mg}$  isotopes. As we can see in Fig.2,  $N = 26$  looks like a new neutron magic number in some intervals of quadrupole deformation. Figure 2 illustrated wide splitting of the single-particle states with increasing deformation and  $\varepsilon_\lambda(\beta_2)$  dependence differs greatly for different  $\lambda$ . In the case of isotopes with  $N = 26, 28$  the  $1f_{7/2}$  state splitting is the most interesting. We can see that upper  $7/2^-$  level occupied by  $N = 27, 28$  is growing rapidly together with  $\beta_2$  and after  $\beta_2 > 0.15$  drip-line nuclides with  $N > 26$  become unbound, for example,  $^{40}\text{Mg}$  and  $^{39}\text{Na}$  (until  $\beta_2 < 0.5$ ). Thus, we can explain the strong discrepancy with the table for heavy magnesium isotopes calculated there in spherical basis.

12			$^{30}\text{Mg}$ 338 ms	$^{31}\text{Mg}$ 236 ms	$^{32}\text{Mg}$ 120 ms	$^{33}\text{Mg}$ 90 ms	$^{34}\text{Mg}$ 20 ms	$^{35}\text{Mg}$	$^{36}\text{Mg}$	$^{37}\text{Mg}$	$^{38}\text{Mg}$	$^{39}\text{Mg}$	$^{40}\text{Mg}$		$^{42}\text{Mg}$
11	$^{27}\text{Na}$ 301 ms	$^{28}\text{Na}$ 31.5 ms	$^{29}\text{Na}$ 43.8 ms	$^{30}\text{Na}$ 50 ms	$^{31}\text{Na}$ 17.2 ms	$^{32}\text{Na}$ 14.0 ms	$^{33}\text{Na}$ 8.1 ms	$^{34}\text{Na}$ 5.0 ms	$^{35}\text{Na}$ 1.5 ms		$^{37}\text{Na}$		$^{39}\text{Na}$		
10	$^{26}\text{Ne}$ 197 ms	$^{27}\text{Ne}$ 32 ms	$^{28}\text{Ne}$ 17 ms	$^{29}\text{Ne}$ 19 ms	$^{30}\text{Ne}$ 7 ms	$^{31}\text{Ne}$ 3.4 ms	$^{32}\text{Ne}$ 3.5 ms		$^{34}\text{Ne}$		$^{36}\text{Ne}^*$				
9	$^{25}\text{F}$ 50 ms	$^{26}\text{F}$ 10.2 ms	$^{27}\text{F}$ 6.5 ms		$^{29}\text{F}$ 2.9 ms		$^{31}\text{F}$		$^{33}\text{F}$						
8	$^{24}\text{O}$ 65 ms		$^{26}\text{O}^*$												
Z/N	16	17	18	19	20	21	22	23	24	25	26	27	28	29	30

Fig. 3. The part of nuclide chart at the region neutron number  $N = 20$  and  $N = 28$ . The deformed nuclei are italicized and spherical nuclei are in roman type. The neutron drip line is shown by solid line. Nuclei (\*) are predicted as quasistationary states ( $A + 2n$ )-type with a lifetime  $\tau \geq 10^{-18}$  s, emitting neutron pair in a weakly bound di-neutron state

On the other hand, the dependence of  $5/2^-$  level occupied by  $N = 26$  on deformation parameter  $\beta_2$  is very weak in this case. But after  $\beta_2 > 0.4$  the  $3/2^+$  level is rising up rapidly from  $1d_{3/2}$  state and  $N = 24$  becomes the drip-line neutron number in small interval of deformation parameters. For example,  $^{33}\text{F}$  may exist as a very deformed nuclide. The case of strong deformations with the parameter  $\beta_2 > 0.5$  is not discussed in this work because self-consistent theoretical approach becomes very complicated here, where various levels ( $1/2^-$ ,  $3/2^+$ ,  $5/2^-$ ) are mixing in a very small energetic interval  $\Delta\varepsilon \sim 1$  MeV for weakly bound system. So the question of particle stability for very deformed  $^{33}\text{F}$  and  $^{36}\text{Ne}$  is still open.

We analyzed the problem of  $N = 28$  magic number from two points of view: from the position of deformation destroying, as was described, the magic  $N = 28$  in our region of nuclei, and from the position of developed pairing in the neutron-rich nuclei. According to STFFS spherical calculations [22] for  $N = 28$  nuclei from  $^{48}\text{Ca}$  to  $^{47}\text{K}$ , the spacing energy  $\Delta\varepsilon$  between the one-particle neutron state  $f_{7/2}$ , which is the highest occupied state in the scheme without pairing, and the unoccupied state  $p_{3/2}$  is rather large ( $\Delta\varepsilon \sim 2.5$  MeV). The gap operator matrix elements is small for these states ( $\Delta_\lambda \sim 0.3$  MeV); therefore, there is no developed pairing in these nuclei. However, for smaller  $Z$  numbers, the situation has strongly changed, and for  $^{46}\text{Ar}$  the  $\Delta_\lambda$  value is more than twice larger, and the level spacing  $\Delta\varepsilon$  decreases as we approach the neutron-stability boundary and falls below 1 MeV

at the drip line. The corresponding matrix elements grow up to  $\Delta_\lambda \sim 1.2$  MeV. Therefore, the number  $N = 28$  loses its magic properties in Mg–Ar region up to the neutron drip line.

### SUMMARY

Nowadays the neutron-rich isotopes  $^{34}\text{Ne}$  and  $^{37}\text{Na}$  have been experimentally observed in the reactions  $^{48}\text{Ca} + \text{natTa}$  [14, 15]. Thus, most probably, the neutron drip line has been reached for the neon and sodium isotopes. However, it seems that to definitely conclude whether these isotopes mark the drip line, further experimental efforts are needed. The neutron-rich  $^{40}\text{Mg}$  with  $N = 28$  has not been observed in these experiments, which can be explained by the deformation effects near the neutron drip line, destroying neutron shell with  $N = 28$ .

According to our microscopic self-consistent calculations with the deformation and pairing effects included, the new neutron drip line was established, and we can see that  $N = 20$  and  $N = 28$  lose their magic properties for very neutron-rich isotopes up to the  $N$  drip line in the O–Mg region. Neutron drip-line number for oxygen neutron-rich isotopes is  $N = 16$ . For a certain region of the quadrupole deformation parameter  $\beta_2$  values, the neutron number  $N = 26$  is a new neutron drip-line number in the considered region of the nuclear map.

On the basis of previous calculations, it was predicted that quasistationary state in  $^{24}\text{O} + 2n$  system may exist as  $^{26}\text{O}^*$  with the width  $\Gamma \sim 10^{-3}$  MeV. Analogously,  $^{36}\text{Ne}^* = ^{36}\text{Ne} + 2n$  and  $^{40}\text{Mg}^* = ^{38}\text{Mg} + 2n$  extra drip-line nuclear quasistationary system may exist with a lifetime  $\tau \geq 10^{-18}$  s, emitting neutron pair in a weakly bound di-neutron state.

**Acknowledgements.** The authors would like to express their gratitude to the members of the FLNR (JINR, Dubna)–GANIL (France) and FLNR (JINR, Dubna)–RIKEN (Japan) collaborations for the fruitful experimental efforts and discussions of the experimental results obtained in the joint experiments. This work has been carried out with financial support from PICS-(IN2P3) No. 1171, grant from INTAS 00-00463 and grant No. 96-02-17381a of the Russian Foundation for Basic Research.

### REFERENCES

1. *Thibault C. et al.* // *Phys. Rev. C.* 1975. V. 12. P. 644.
2. *Lutostansky Yu. S., Zverev M. V., Panov I. V.* // *Proc. of the 5th Intern. Conf. on Nuclei Far from Stability*, Canada, 1987. *Am. Inst. of Phys. N. Y.*, 1988. P. 727; *Izv. AN USSR.* 1989. V. 53. P. 849.
3. *Guillemaud-Mueller D. et al.* // *Z. Phys. A.* 1989. V. 332. P. 189.
4. *Guillemaud-Mueller D. et al.* // *Phys. Rev. C.* 1990. V. 41. P. 937.
5. *Tarasov O. B. et al.* // *Phys. Lett. B.* 1997. V. 409. P. 64.
6. *Fauerbach M. et al.* // *Phys. Rev. C.* 1996. V. 53. P. 47.
7. *Sakurai H. et al.* // *Ibid.* V. 54. P. R2802.
8. *Sakurai H. et al.* // *Phys. Lett. B.* 1999. V. 448. P. 180.
9. *Campi X. et al.* // *Nucl. Phys. A.* 1975. V. 251. P. 193.

10. Nayak R., Satpathy L. // Nucl. Phys. A. 1978. V. 304. P. 64.
11. Poves A., Retamosa J. // Nucl. Phys. A. 1994. V. 571. P. 221.
12. Warburton E. K., Becker J. A., Brown B. A. // Phys. Rev. C. 1990. V. 41. P. 1147.
13. Sorlin O. *et al.* // Phys. Rev. C. 1993. V. 47. P. 2941.
14. Notani M. *et al.* // Phys. Lett. B. 2002. V. 542. P. 49.
15. Lukyanov S. *et al.* // J. Phys. G. 2002. V. 28. P. L41.
16. Moller P. *et al.* // At. Data Nucl. Data Tables. 1995. V. 39. P. 185.
17. Lalazissis G. A. *et al.* // Phys. Rev. C. 1999. V. 60. P. 014310.
18. Caurier E. *et al.* // Phys. Rev. C. 1998. V. 58. P. 2033.
19. Ren Z. *et al.* // Phys. Rev. C. 1995. V. 52. P. R20.
20. Terasaki J. *et al.* // Nucl. Phys. A. 1997. V. 621. P. 706.
21. Lalazissis G. A. *et al.* // Phys. Rev. C. 1999. V. 60. P. 014310.
22. Zverev M. V. *et al.* // Phys. of Atomic Nucl. 1995. V. 58. P. 2058.
23. Zverev M. V., Saperstein E. E. // Yad. Fiz. 1984. V. 39. P. 1390.
24. Zverev M. V., Saperstein E. E. // Yad. Fiz. 1985. V. 42. P. 1082.
25. Starodubsky V. E., Zverev M. V. // Yad. Fiz. 1991. V. 54. P. 676.
26. Kromer E. *et al.* // Phys. Lett. B. 1995. V. 363. P. 12.

Received on November 5, 2002.